



The primary energy estimation of inclined giant EAS

J.-N. Capdevielle, F. Cohen, B. Szabelska, J. Szabelski

► To cite this version:

J.-N. Capdevielle, F. Cohen, B. Szabelska, J. Szabelski. The primary energy estimation of inclined giant EAS. 20th European Cosmic Ray Symposium - ECRS 2006, Sep 2006, Lisbonne, Portugal. in2p3-00144680

HAL Id: in2p3-00144680

<https://hal.in2p3.fr/in2p3-00144680>

Submitted on 4 May 2007

HAL is a multi-disciplinary open access archive for the deposit and dissemination of scientific research documents, whether they are published or not. The documents may come from teaching and research institutions in France or abroad, or from public or private research centers.

L'archive ouverte pluridisciplinaire **HAL**, est destinée au dépôt et à la diffusion de documents scientifiques de niveau recherche, publiés ou non, émanant des établissements d'enseignement et de recherche français ou étrangers, des laboratoires publics ou privés.

The primary energy estimation of inclined giant EAS

Jean Noel Capdevielle
and Fabrice Cohen

APC, Université de Paris 7, 10 rue Alice Daumont
70025 Paris Cedex 13, France
Email: capdev@apc.univ-paris7.fr

Barbara Szabelska
and Jacek Szabelski

The Andrzej Soltan Institute for Nuclear Studies,
Cosmic Ray Laboratory
90-950 Lodz 1, POBox 447, Poland

Abstract—Determination of the primary energy by surface arrays (like AGASA) through estimators (instead of total size), taken as densities at 600 m from the shower axis, needs a special procedure for inclined cascades when the maximum is close to the array (less than 2-3 radiation lengths above). According to the cascade theory and the simulations with the CORSIKA code above 10 EeV the exponential function used for $\rho(600)$ conversion from inclined to vertical showers is no longer valid. As follows from simulations at energies near to 100 EeV, the density at 600 m for zenith angles 25-35° exceeds by 10% the vertical density, whereas it was assumed to be 30% lower in the previous treatments. Such treatments generate an artificial increase in the estimation of the primary cosmic ray energy. The primary spectrum reconstructed by an appropriate procedure for inclined showers confirms GZK prediction and eliminates the divergence between measurements at ultra-high energies.

I. INTRODUCTION

An important discrepancy in the determination of the primary energy spectrum above 10^{19} eV was underlined in 2001 [1] between the data of HiRes collected by the atmospheric fluorescence and the data accumulated by the very large surface array of AGASA. The results of HiRes based on the registration of the longitudinal development exhibited a tendency in agreement with GZK prediction. This tendency is confirmed by the recent compilation of HiRes 1, 2 and HiRes stereo [2].

Last year we pointed out [3], [4] that the primary energy in the surface array was mainly overestimated by reason of an inappropriate conversion of the energy estimation, i.e. the density, $\rho_{600}(\Theta)$ to the vertical density $\rho_{600}(0^\circ)$, for giant inclined showers. Recently, the group of AGASA has reduced the intensity of ultra-high energy [5] and a new calibration of the raw data is in progress in the direction of a more complete reduction.

We review here the problem of energy estimation for inclined showers taking into account the results of our simulations. A general method suitable for the scientific problems related to the absorption versus zenith angle above 10^{19} eV is proposed.

II. APPROACH OF THE PRIMARY ENERGY FROM THE SIZE N IN AKENO

The arrangement of scintillators in original Akeno air shower experiment [6] was covered over an approximate area

of 1 km^2 and was characterized by a general spacing of 120 m. The configuration of detectors was reduced to 30 m in 3 regions, each of area $(90 \times 90) \text{ m}^2$. The configuration of 1 km^2 included a total of 156 scintillators with 1 m^2 area to measure the differential size spectrum $J(N)$ at 920 gcm^{-2} and to derive the primary flux $J(E_0)$ up to $10^{18.8} \text{ eV}$. The lateral distribution of charged particles used in Akeno [6] for very large shower is the sum of one pair of NKG functions and the size N is derived from the densities by integration over the area.

The size is then converted to the primary energy for $(10^6 \leq N \leq 10^9)$ following [6]:

$$\bar{E}_1(\text{eV}) = 3.9 \times 10^{15} \times \left(\frac{N}{10^6} \right)^{0.9}. \quad (1)$$

We have verified that this relation applied for vertical showers coincides with the results of CORSIKA [7] (version 6.16, proton primaries, QGSJET model [8]) within 2% around 10^{18} eV [9].

In the case of inclined showers, an average attenuation length can be expressed by $\Lambda_e = 204 \text{ gcm}^{-2}$ for a zenith angle $\Theta \leq 45^\circ$ and the relation between inclined and vertical size for the same primary particle energy can be written as:

$$N(\Theta) = N(0) \times \exp \left(-\frac{(t - t_0)}{\Lambda_e} \right) \quad (2)$$

with $t = t_0 \sec(\Theta)$ and $t_0 = 920 \text{ gcm}^{-2}$. This attenuation length is also in agreement with the longitudinal development calculated with CORSIKA [10], [9]. After correction for the dispersion in zenith angle determination, the fluxes plotted in Fig. 1 have been obtained and expressed by a power law:

$$J(E_0) = A \times \left(\frac{E_0}{E_c} \right)^{-\gamma}. \quad (3)$$

This method was applied to events with energy up to $5 \cdot 10^{18} \text{ eV}$.

III. APPROACH OF THE PRIMARY COSMIC RAY SPECTRUM FROM THE DENSITIES IN GIANT SURFACE ARRAYS

A. Charged particle densities and scintillator arrays

The 20 km^2 array (Array 20) which was constructed before the AGASA experiment, consisted of 19 detectors (individual area of the detector 2.25 m^2), separated by about 1 km from

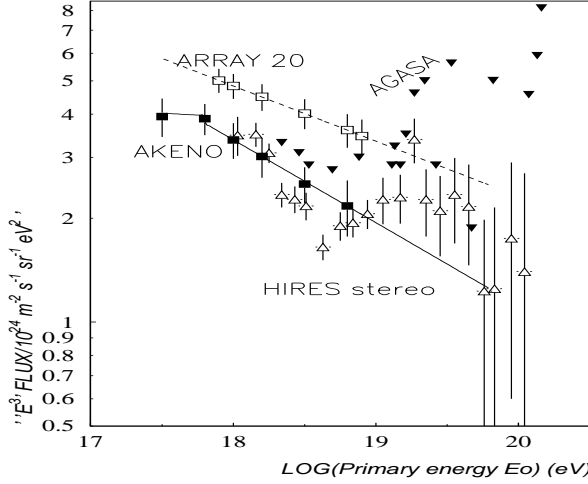


Fig. 1. Differential primary spectrum for Array 1 (Akeno), Array 20, AGASA and HiRes Stereo experiments. Array 1 or Akeno (full squares) concerns the data of the 1 km² array before 1992. Array 20 (open squares) concerns the earliest data of the 20 km² array. AGASA (full triangles) is the data of the 100 km² array in 2003 and HiRes Stereo labels the Stereo data in 2003 (open triangles). Also shown are the fitted spectra, for Akeno (full line) and Array 20 (dashed line). For the clarity of the graph, the error bars are not plotted for AGASA data.

each other. The array involved 4 detectors inside the 1 km² area of Akeno. The registration of giant EAS with very large distances between the detectors gives statistically more chances to record low densities at large distance from the core. Furthermore, the detectors inside about 2 Moliere radii from the axis are usually saturated. The Particle Data Group (PDG) estimates that 1% only of the cascade energy lies outside a cylinder of 3.5 Moliere radii [11]. A direct access to the total size N from the densities becomes hopeless and a common procedure, the conversion of the density near 600 m from the axis, was introduced as a preliminary energy estimator [12]. This method is very sensitive to axis localization accuracy, as the lateral distribution is decreasing rapidly with distance [24].

In such context, the lateral distribution for the Array 20 has been selected as follows [16]:

$$\rho(r) = N C_e x^{-\alpha} (1+x)^{-(\eta-\alpha)} \left(1 + \frac{r}{2000}\right)^{-0.5} \quad (4)$$

(C_e being a normalization constant). This analytic description with a fixed value $\alpha = 1.2$, without reference to the age parameter is used to determine the shower axis and to interpolate the value of the density at 600 m. In contrast to the size conversion in Array 1, the scintillator response in terms of density S_{600} is here converted to the primary energy following:

$$E_{20}(\text{eV}) = 2.0 \cdot 10^{17} \times (S_{600})^{1.0}. \quad (5)$$

This energy estimation takes into account the relation between S_{600} and $\rho(600)$ following calibrations with the arrays of

Haverah Park and Yakutsk [13]. The quantity $S(r)$ can be related to the electron and muon densities [14] following:

$$S(r) = \frac{(\rho_e(r) + \rho_\mu(r)k_\mu(r))}{k_{array}} \times k_{sc}(r) \quad (6)$$

with $k_\mu(r) = 1.8(E_\mu \geq 1\text{GeV})$, $k_{sc}(r) = 1.4$ (for $r = 600$ m) and $k_{array} = 1.1$. The original values were obtained in Akeno by comparing the acceptance of Array 20 to Array 1 as $k_{array} = 1.1$ and from comparison of scintillator densities to spark chamber densities as $k_{sc}(r) = 1.1$. This last value was underestimated at large distances and a value of 1.4 has to be taken at 600 m from the axis [14]. From a set of 40 vertical showers simulated with CORSIKA (proton primaries, GHEISHA option) at 10^{18}eV , we obtain at 600 m the average electron and muon densities of 3.3 and 1.2 respectively. The value $k_\mu(r) = 1.8$ has been obtained from the muon densities recorded for $E_\mu \geq 1\text{GeV}$ at 600 m distance by the muon detectors contained in Array 20. Taking into account the energy thresholds for electrons and muons in CORSIKA (1.5 and 300 MeV respectively), we have inserted in formula 6 ρ_e and ρ_μ for 600 m, attributing to $k_\mu(600)$ a value 1.4 (given by our muon energy spectrum from CORSIKA [9]). This conversion by formula 6 in those conditions appears to overestimate the primary energy by about 20%, even if we select the FLUKA or UrQMD options of CORSIKA [9], [15], which are more favourable than the GHEISHA option. The average electron and muon densities from CORSIKA return here via relation (5) $E_0 = 1.26 \cdot 10^{18}\text{eV}$, respectively $1.19 \cdot 10^{18}\text{eV}$ for Fluka, instead of the primary energy $E_0 = 10^{18}\text{eV}$ set in our simulation. In other words, we received from our simulation (CORSIKA, option UrQMD) an average density $S_{600} = 6.0$ from equation (6) involving the average electron and muon densities calculated, when $S_{600} = 5.0$ was expected according to the conversion of Array 20; this minimal overestimation of the primary energy by about 20% remains approximately constant up to 10^{20}eV by reason of the quasi-linear dependence of S_0 on S_{600} .

B. Energy estimators for giant EAS

In place of the size spectrum, the S_{600} differential spectrum in Array 20 is obtained taking an attenuation length Λ_{600} in parallel to Λ_e in Array 1 following:

$$S_{600}(\Theta) = S_{600}(0) \times \exp\left(-\frac{(t-t_0)}{\Lambda_{600}}\right). \quad (7)$$

A constant value $\Lambda_{600} = 500\text{gcm}^{-2}$ was assumed according to the best fit value on the zenith angle distribution for constant S_{600} adjusted by the simulations [13] for different Λ_{600} .

This conversion used in the Akeno 20 array [16] was considered as valid up to $\sec(\Theta) = 1.4$. The determination of the attenuation curve of S_{600} by the method of "equal intensity cuts", including experimental data recorded for showers with larger zenith angles (up to 60°), demonstrated later significant deviations for $\sec(\Theta) > 1.4$.

An improved and more general conversion (valid also for

$sec(\Theta) > 1.4$ was inferred by fitting the attenuation of S_{600} up to $sec(\Theta) = 1.7$ [17] represented by:

$$S_{600}(\Theta) = S_{600}(0) \times \exp \left(-\frac{t_0}{\Lambda_1} (sec(\Theta) - 1) - \frac{t_0}{\Lambda_2} (sec(\Theta) - 1)^2 \right) \quad (8)$$

with $\Lambda_2 = 594^{+268}_{-130} \text{ g cm}^{-2}$.

This relation 8 was finally used in the treatment of AGASA data with $\Lambda_1 = 500 \text{ g cm}^{-2}$ [18], introducing minor changes for $sec(\Theta) < 1.4$.

IV. $S_{600}(\Theta)$ VERSUS $S_{600}(0)$ WITH CORSIKA ABOVE 10^{19} eV

A. Simulations

Simulations with CORSIKA code have been performed for gammas, protons and iron nuclei as primary particles for 6 energies and in most cases for 8 different zenith angles. The observation level corresponded to the Auger experiment. 40 EAS have been simulated for each combination of primary particle, energy and zenith angle [10].

From simulations we have obtained the total number of particles in EAS at observation level N_{tot} as a function of zenith angle Θ for gammas (energy above 2 MeV), electrons-positrons, and muons. N_{tot} was estimated in the CORSIKA program using fits to longitudinal development. We used these estimations present in results of simulations. Presented here values are average numbers from 40 EAS.

In the Fig. 2 we present N_{tot} (e^+e^- only) as a function of $sec(\Theta)$ for each primary particle type. The energies of primary particles are indicated. The dashed line is proportional to AGASA conversion of particle density at 600 m from zenith angle Θ to the corresponding value for vertical shower (formula 7).

B. Fit with distorted gaussian function

We have pointed out [3] from the total data simulated above 10^{19} eV , an important change of the behavior of $S_{600}(\Theta)$ versus $sec(\Theta)$. Instead of the classical decrease of the absorption regime of relation 8, the density increases progressively in function of the primary energy versus $sec(\Theta)$ reaching a maximum between $10 - 20^\circ$ and then decreases with zenith angle as shown in Fig. 3 for primary protons for $E_0 = 10^9, 5 \cdot 10^9, 10^{10}, 5 \cdot 10^{10}, 10^{11} \text{ GeV}$. Such situation in the case of AUGER corresponds to a maximum depth of the longitudinal development at about one electron radiation length (for $E_0 = 10^{11} \text{ GeV}$) above the experimental array (a similar situation in AGASA would be obtained with a model of modest multiplicity such as HDPM). For a model with large multiplicity, such as QGSJET2, the same maximum is near 3 electron radiation lengths above AGASA and the total discrepancy is slightly reduced but still appreciable (Fig. 3). This typical behavior can be described analytically by the so called distorted gaussian

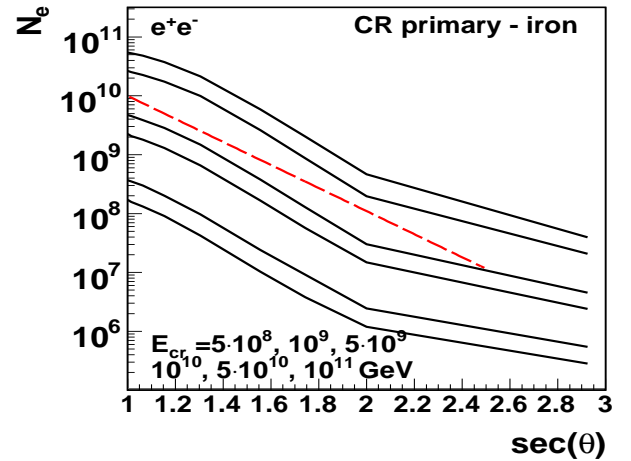
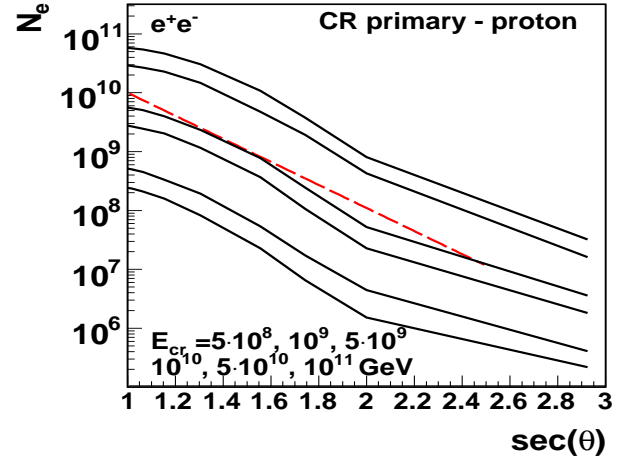
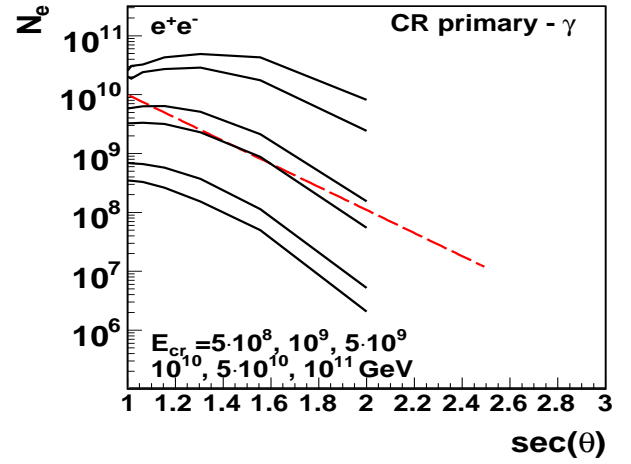


Fig. 2. Total number of particles (e^+e^-) in EAS versus $sec(\Theta)$ for primary photon, proton and iron. Primary energies are indicated. The broken line is Akeno formula 2 for $N(\Theta)$ with normalization to $N(0) = 10^{10}$.

function:

$$f(l) = A \times \exp \left(\frac{k}{8} - \frac{s\delta}{2} - \frac{1}{4}(2+k)\delta^2 + \frac{1}{6}s\delta^3 + \frac{1}{24}k\delta^4 \right) \quad (9)$$

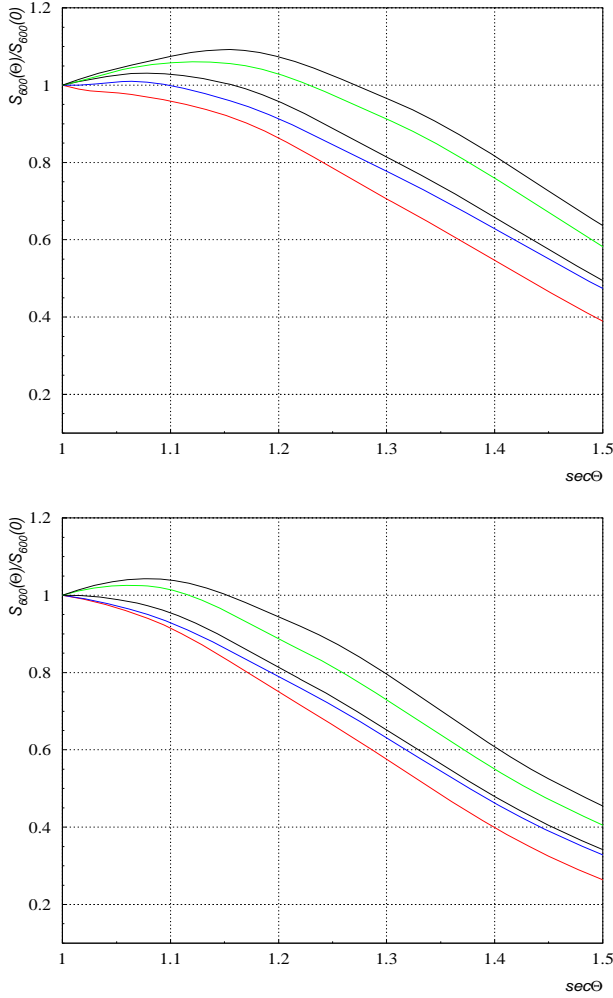


Fig. 3. Relative dependence $\frac{S_{600}(\Theta)}{S_{600}(0)}$ versus $\sec(\Theta)$ for protons of primary energy $E_0 = 10^9, 5 \cdot 10^9, 10^{10}, 5 \cdot 10^{10}, 10^{11}$ GeV (from bottom to top) respectively for interaction models of high multiplicity (lower part) and low multiplicity (upper part)

where:

$$l = \sec(\Theta), \delta = (l - \langle l \rangle) / \sigma, \sigma^2 = \langle l^2 \rangle - \langle l \rangle^2$$

$$s = \langle (l - \langle l \rangle)^3 \rangle / \sigma^3 \text{ skewness}$$

$$k = \langle (l - \langle l \rangle)^4 \rangle / \sigma^4 \text{ kurtosis}$$

Values of parameters in formula 9 for different energies are summarized in the Table I for the interaction models with low multiplicity and in the Table II for interaction models with high multiplicity.

The depths of the experimental array taken in the calculations are respectively 860 gcm^{-2} for AUGER and 920 gcm^{-2} for AGASA.

The dependence shown in the Fig.3 is a general consequence of the electromagnetic cascade theory. This can be illustrated easily, at least quantitatively by the behavior of NKG curves just after maximum for $s > 1$, as shown a long time ago [19]. Even if the total size decreases, for small densities, at about 2 Moliere radii from axis for showers of 10^6 GeV recorded, for

TABLE I
TABLE OF COEFFICIENTS $A, \langle l \rangle, \sigma, s$ AND k VERSUS ENERGY FOR LOW MULTIPLICITY MODEL AT AGASA LEVEL OR FOR HIGH MULTIPLICITY MODEL AND AUGER LEVEL

E_0 (eV)	A	$\langle l \rangle$	σ	s	k
10^{20}	1.1	1.159	0.339	$0.143 \cdot 10^{-5}$	$0.832 \cdot 10^{-1}$
$5 \cdot 10^{19}$	1.06	1.146	0.341	$0.244 \cdot 10^{-5}$	0.158
10^{19}	1.032	1.090	0.345	$0.300 \cdot 10^{-4}$	0.104
$5 \cdot 10^{18}$	1.011	1.029	0.384	$0.242 \cdot 10^{-6}$	$0.191 \cdot 10^{-2}$
10^{18}	1.0	0.998	0.368	$0.179 \cdot 10^{-5}$	$0.203 \cdot 10^{-1}$

TABLE II
TABLE OF COEFFICIENTS $A, \langle l \rangle, \sigma, s$ AND k VERSUS ENERGY FOR HIGH MULTIPLICITY MODEL AT AGASA LEVEL

E_0 (eV)	A	$\langle l \rangle$	σ	s	k
10^{20}	1.0	1.155	0.310	$0.214 \cdot 10^{-3}$	0.550
$5 \cdot 10^{19}$	1.0	1.109	0.312	$0.278 \cdot 10^{-6}$	0.968
10^{19}	1.0	1.029	0.337	$0.764 \cdot 10^{-4}$	0.337
$5 \cdot 10^{18}$	1.0	1.012	0.339	$0.119 \cdot 10^{-2}$	0.341
10^{18}	1.0	1.016	0.310	$0.323 \cdot 10^{-1}$	0.963

instance at Chacaltaya, the density will increase with zenith angle before decreasing above 30° . In our simulation with CORSIKA, in spite of the limits of validity of cascade theory (we are dealing with distances of about 7 Moliere radii), those comparable consequences result from the effect of the multiple Coulomb scattering as described in EGS and implemented in CORSIKA.

V. INDUCED DIVERGENCE IN THE PRIMARY SPECTRUM

We have simulated several groups of two millions of EAS above 10^{18} eV with an E^{-3} spectrum and examined the reconstruction following the procedure used by AGASA. Both primary energy and zenith angle are generated. The vertical density at 600 m from the axis is first sampled from the distribution derived from our CORSIKA data bank. This density is transformed to density $S_{600}(\Theta)$ by interpolation on the primary energy in relation 9. This density is then converted to $S_{600}(0)$ following the treatment of AGASA through the formula 8 from zenith angle Θ to the corresponding value for vertical shower (formula 8). In the last step, the primary energy E_0 (in eV) is recovered with the conversion of AGASA [5]:

$$E_0 = 1.96 \cdot 10^{19} \times \left(\frac{S_{600}(0)}{100} \right)^{1.02} \quad (10)$$

For both configurations of Fig. 3, the divergence at ultra high energy introduced artificially in the primary spectrum can be ascertained (Fig.4)

In both parts of the Fig. 4 we present the same results on the reconstructed spectrum: in the upper part differential intensity multiplied by E^3 and in the lower part differential intensity. In both cases a cut off at 10^{20} eV has been introduced in the

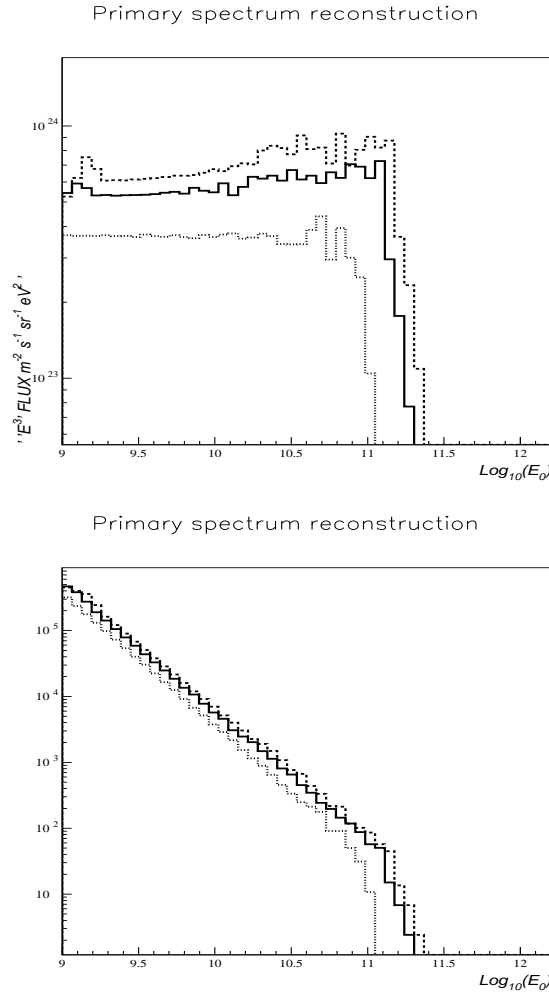


Fig. 4. Differential energy spectrum generated as E^{-3} for $2 \cdot 10^6$ showers (on lower histogram with dotted line) and reconstructed respectively for interaction models of high multiplicity and low multiplicity. The upper histogram (dashed line) corresponds to the Table I (solid line), associated to the Table II is in the middle.

generation of the original spectra. We notice the increase of the spectrum above $2 \cdot 10^{19}$ eV as well as the generation of showers above the energy cut off. The energy overestimation versus zenith angle is general and especially important in all the circumstances where the curves of Fig. 3 are above the unity; the density $S_{600}(\Theta)$ is systematically multiplied by a factor larger than 1 derived from equation 8 whereas it has to be divided by a factor larger than 1 interpolated versus E_0 in the Fig. 3 or with our distorted gaussian function. It can be seen in Fig. 3 that such situation happens at $5 \cdot 10^{19}$ eV between $0^\circ - 27^\circ$ and at 10^{20} eV between $0^\circ - 30^\circ$. This overestimation affects 62% and 73% of the data contained in the solid angle inside 45° at $5 \cdot 10^{19}$ eV and 10^{20} eV respectively, included in the spectrum of AGASA. In the case of the 2nd set of parameters (Table II), those proportions are slightly reduced, respectively to 36% and 44%.

Despite the suppression of the energy generation above

100 EeV, the simulation shows that the treatment of AGASA artificially generates events up to 200 EeV. With additive fluctuations (uncertainty in axis localisation, fluctuations of detector's responses...), we have ascertained that this bias at ultra high energy could even increase. An extended simulation of 200 million showers without upper energy cut off confirmed those features as shown in the Fig. 5. Turning to a more actual generation procedure, we have selected the spectrum described by 3 power laws introduced by Bergman [21]; the results of the Monte Carlo generation are displayed on the lower part of Fig. 5 and they reflect a discrepancy exhibiting several similarities with the experimental polemics between AGASA and HiRes.

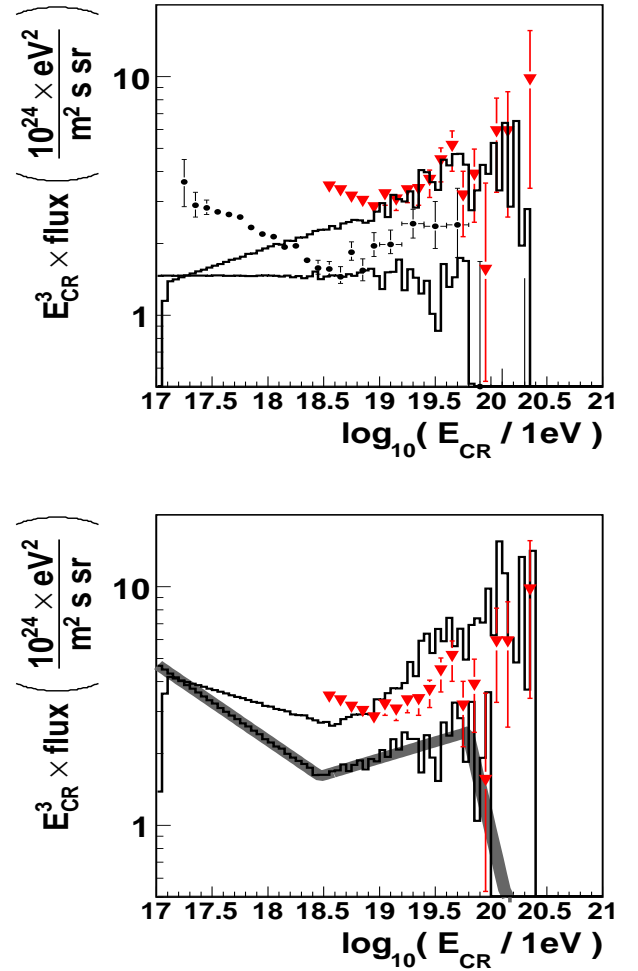


Fig. 5. Upper part: black circles are HiRes-2 Monocular energy spectrum [2] and red triangles show AGASA spectrum [2]. Lower histogram is the CR energy spectrum generated from E^{-3} distribution without energy cut off with 1000 events above 10^{19} eV and normalized to HiRes spectrum at 10^{19} eV. Upper histogram was obtained from events generated assuming isotropy ($\Theta < 60^\circ$) and AGASA method: eq. 5, top Figure 3 and Table I. Lower part: Bergman's [21] spectrum with 3 power laws (grey band) was used for generation limited to 1000 events above 10^{19} eV. Normalization to Bergman's spectrum was applied to lower histogram. Upper histogram was obtained using AGASA method.

Again, in the 3 parts of this spectrum (3 power laws with an exponent $\gamma = 3.12, 2.86, 5.$ respectively for $\text{Log}(E_0) \leq 18.47, \leq 19.79$ and ≥ 19.79), the energy overestimation is also generated in a proportion similar to the discrepancy between AGASA and HiRes in Fig. 1.

VI. DISCUSSION

A. Earliest discrepancies between Akeno and AGASA

The intensity excess by a factor 1.5 of the primary spectrum obtained with Array 20 in the overlapping region when compared to Akeno (the corresponding points are plotted in Fig. 1, together with the best fit following the adjustment [16]) was immediately explained by the different methods used for the primary energy reconstruction in each array. A discrepancy by a factor 1.15 in the primary energy derived from equation 5 instead of equation 1 was pointed out and considered as in agreement with the energy determination via S_{600} in the experiments of Haverah Park and Yakutsk. Those ambiguities have been treated later [18] in terms of systematic errors on detectors response versus zenith angle, seasonal variance and other complex problems related to the shower selection and the collecting area.

The more recent values reported by AGASA [25] are closer to the values of Akeno than the values of Array 20 (Fig. 1); the intensities of AGASA remain, however, larger than for Array 1 in the overlapping energy region and exhibit a general excess by 30% when compared to HiRes Stereo data.

B. Attenuation length for the energy estimator

From our simulation data, we have derived the values of the attenuation length Λ_{600} for different zenith angles (Fig. 2); for small inclinations $\Theta \leq 30^\circ$ the values of the attenuation length concerning proton primaries are quite more important than the average value $\Lambda_{600} = 500 \text{ gcm}^{-2}$ used in AGASA. When the primary energy is increasing, the depth of the maximum becomes more and more close in altitude to the arrays, such as AUGER or AGASA: the conversion of inclined densities to $S_{600}(0)$ according to equation 8 becomes poorly appropriate as the cascade is far from a stable absorption phase, especially for proton primaries. In the depth interval of about 5 radiation units following the maximum, we can summarize the absorption process as follows:

- the total size N is decreasing slowly versus the atmospheric depth t
- the age parameter increases in parallel from 1.0 up to 1.2
- the lateral distribution around 600 m from the axis becomes flatter [9]

The increase of the flattening of the density distribution turns to a systematic overestimation (via relation 8) of the vertical density which influences the primary energy. The shower recorded might be classified in bins of larger energy. The values of Λ_{600} derived from lines presented in the Fig. 6 will increase for energies lower than $2 \cdot 10^{19} \text{ eV}$ (at higher energy there is no more classical exponential absorption). The experimental points in the Fig. 6 suggest indeed at the highest

energy the suppression of the absorption with a maximum of S_{600} against Θ resulting from the method of the constant intensity cuts. The overestimation of the primary energy from the densities converted by formula 8, using 500 gcm^{-2} instead of 2000 gcm^{-2} in the overlapping region for $\Theta = 20^\circ$ is about 10%. The adaptation of the conversion of the densities of inclined showers, the ambiguities on the scintillator response and the relation 8 can probably explain the discrepancies of 30% between HiRes and AGASA (Fig. 1) for energies below $2 \cdot 10^{19} \text{ eV}$.

Above $3.5 \cdot 10^{19} \text{ eV}$ a clear divergence in the discrepancies between AGASA and HiRes Stereo appears rising from 150% to above 300% at $6 \cdot 10^{19} \text{ eV}$. This may come again from the lateral distribution becoming flatter more rapidly than the reduction of the total size: the net result is that the densities (at 600 m) are 5-10% larger in the bin $\Theta = 20^\circ - 30^\circ$ than the vertical density when the atmospheric depth separating the array and the shower maximum becomes lower than 3 cascade units. Additionally the inaccuracy of position of shower axis determination can contribute here [24] as the relation 4 is constant in the central part (α is fixed to 1.2), with consequences on the estimator S_{600} .

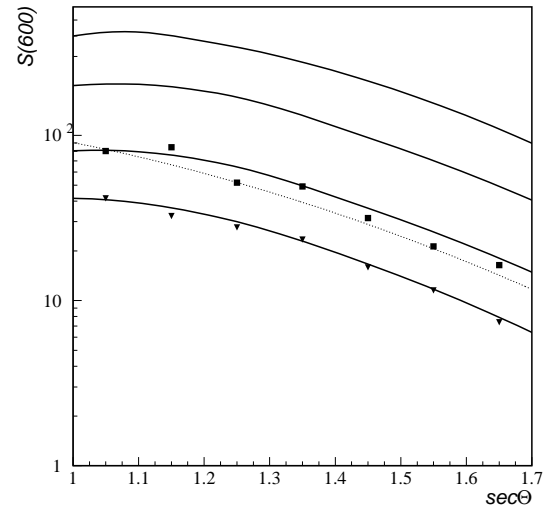


Fig. 6. Attenuation length of S_{600} for $\Theta = 10^\circ - 50^\circ$ compared to the earliest measurements (method of constant intensity cuts) and description of AGASA [17]. $E_0 = 10^{19}, 2 \cdot 10^{19}, 5 \cdot 10^{19}, 10^{20} \text{ eV}$ (from the bottom to the top)

C. Influence of the primary composition

Relation of the S_{600} estimator versus zenith angle in the neighbourhood of the maximum is complex and depends also on the primary composition. In the Table III we have reported the relative dependence on zenith angle at 10^{20} eV for $s(\Theta) = S_{600}(\Theta)/S_{600}(0)$ and $\delta_{vme}(\Theta) = \Delta_{vme}(\Theta)/\Delta_{vme}(0)$ in the case of water Cerenkov tanks, like in Haverah Park or AUGER, for vertical muon equivalents ($\Delta_{vme}(\Theta)$ is the

average density of vertical muons equivalent recorded at the distance considered, here 600 m).

TABLE III

RELATIVE DEPENDENCE OF ESTIMATORS AT 600 M ON ZENITH ANGLE FOR PROTON AND IRON PRIMARIES AT 10^{20} eV. THE RATIO TO THE VERTICAL DENSITIES ARE TABULATED FOR SCINTILLATORS ($s(\Theta)$) AND WATER CERENKOV DETECTORS ($\delta_{vme}(\Theta)$)

Θ	10°	20°	30°	40°	50°
$s(\Theta)$, p	1.05	1.08	1.17	1.0	0.65
$s(\Theta)$, Fe	1.01	1.01	0.94	0.80	0.47
$\delta_{vme}(\Theta)$, p	1.06	1.09	1.13	1.02	0.70
$\delta_{vme}(\Theta)$, Fe	1.01	1.01	0.97	0.83	0.53

From our Monte Carlo calculation, we found the maximal increase of the S_{600} densities near 30° for protons, equal to 17% for scintillators and 12.6 % for water Cerenkov tanks (those proportions are average quantities for groups of 40 showers). This can be the origin of an overestimation of the primary energy in comparable proportions.

For iron primaries, the situation is more stable but the average excess in vertical density, $S_{600}(0)$ or $\Delta_{vme}(0)$, is respectively 26% and 30% as compared to vertical protons: this discrepancy decreases when Θ increases with similar values of the estimators at 30° for scintillators and at 45° for the water Cerenkov tanks. The conversion to the primary energy for scintillators is then comparable for protons and heavy primaries only near 30° ; the relation 8 provides an inappropriate description for the absorption generating an energy overestimation for protons in the band 10° - 40° and a constant overestimation up to 30° for iron primaries.

On the contrary the error on the localizations of the estimators at 800 m or 1000 m do not change the situation for a heavy primary component; $s(0)$ and $\delta_{vme}(0)$ are increasing similarly, by 26% and 30% respectively at each distance, when passing from proton to iron. (Those values are obtained from the respective densities at axis distances of 800 m and 1000 m). Furthermore, for iron, s and δ_{vme} do not depend on Θ up to 30° .

In the case of protons, the maximal enhancement near 30° appears reduced at 800 m from the axis (11% for both s and δ_{vme} instead of 26% at 1000 m). For giant showers and detectors separation by 1000 m or more, the accuracy on the density interpolation might be improved (a larger number of detectors hit are located at distances lower than 800 m) and there could be some advantages to move the estimator at 800 m.

D. How to amend AGASA data?

It is difficult to trace back the characteristics of the showers used to build the primary spectrum presented by AGASA. An experimental zenith angle distribution is needed after correction of all possible bias. At ultra high energy, due to

the low statistics and corrections being still in progress, it is not available. To illustrate an approach of rescaling the data, we have generated a primary spectrum following one analytic description commonly used by the group of AGASA [18]: the differential spectrum is approximated by two power laws, as in equation 3 with a first exponent $\gamma_1 = 3.2$ for $E_0 \leq 10^{19}$ eV and a second exponent $\gamma_2 = 2.3$ at larger energies (Fig. 7). For each primary energy generated, the vertical density is derived via relation 10; the angle Θ is then generated randomly inside 45° (we underline that this step is a pure assumption neglecting the registration conditions and non adapted to the low statistics of events at ultra high energy).

The corresponding $S_{600}(\Theta)$ is then derived by relation 8 with a statistic weight $\sin(\Theta)$ taking into account the size of the elementary solid angle. The assumed correct energy (obtained via relation 9) is then sorted in the adequate energy bin. The corrections near to 10^{20} eV would reach a factor of

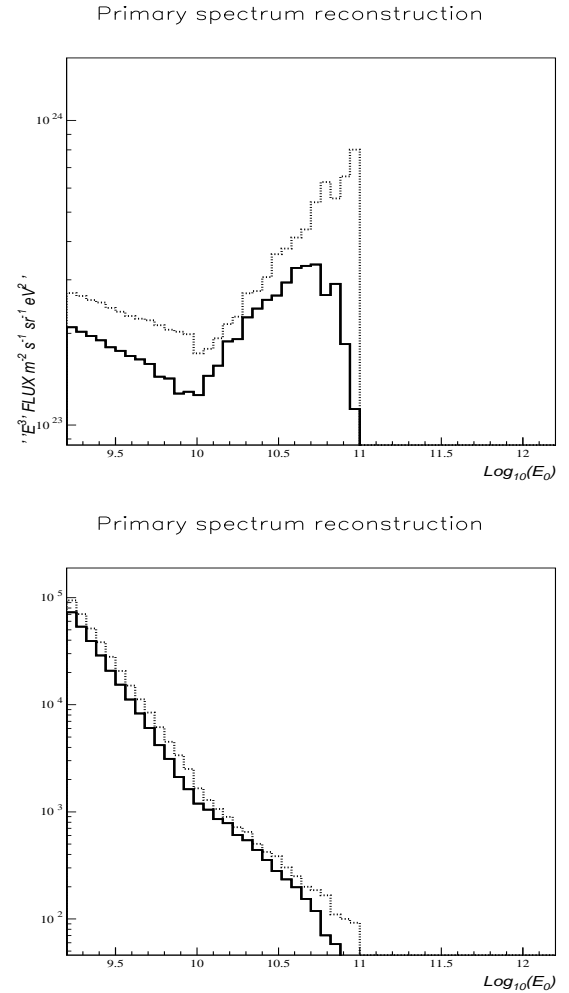


Fig. 7. Upper part: Intensity multiplied by E^{-3} generated for AGASA spectrum fitted with 2 power laws (dotted line) and amended (solid line). Lower part: Differential spectra in the same conditions. Statistics obtained from the simulation of $2 \cdot 10^6$ showers. The solid lines are obtained with the assumptions of Table I

reduction by 7-10, if we consider a large number of showers in each energy bin converted by our procedure. This procedure is not valid for a limited number of showers and the experimental data must be sorted again in the convenient bins of energy and zenith angle event per event. Such work can be performed correctly only with the raw data of the experimentators. Revision is now in progress by AGASA group [5] going along formula 8, as previously suggested by us [3], [4]. Half of the events above 100 EeV have been already rejected [5] and the present intensities look more close to the measurements of HiRes.

A very speculative solution to the problem is shown in the Fig. 8. AGASA energy spectrum from the Fig. 1 has been repositioned bin by bin according to the factors obtained from the Fig. 7. The oversimplifications of the procedure could make dubious the claim of a quantitative correction of AGASA spectrum and we exhibit hereafter a simple tendency of the reduction expected. Conserving in mind the limits and weak points of the statistical treatment, we observe, however, a reasonable and encouraging tendency...

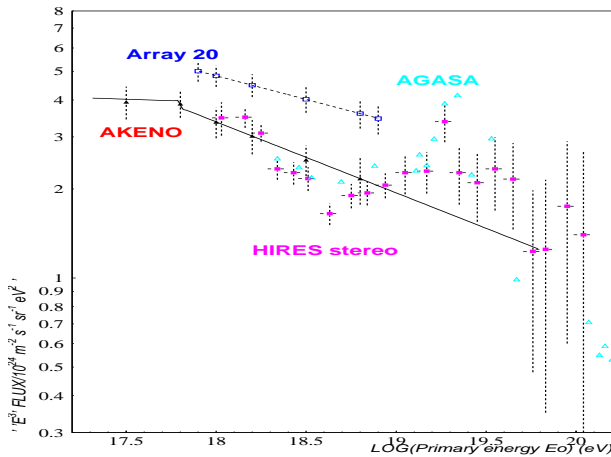


Fig. 8. Differential primary spectra for Akeno, Array 20, HiRes as in Fig. 1 with a conjectural position of AGASA points. The conversion of AGASA points is rather one of the possible tendencies than a precise correction by reason of the oversimplified and speculative treatment, as indicated in the text.

VII. CONCLUSION

An impressive data of high quality has been collected in AGASA. Further simulations with CORSIKA, even with fastened versions (hybrid Monte carlo and analytic codes) to estimate more carefully the array response with a huge statistics, completed by simulations with GEANT for the scintillator response and carried in close contact with the experiment, may help to clarify in detail the discrepancies between the surface arrays and the fluorescence observatories. The present approach points out a better consistency between the spectra obtained by classical size measurements and HiRes Stereo measurements, but also the possibility to amend the AGASA spectrum by an adequate procedure determining the

primary energy of inclined showers. This tendency favours the GZK prediction and after a suitable correction of AGASA data, a general convergence towards the GZK prediction can be expected.

New estimations of the attenuation length by the classical approach of the constant intensity cuts method (applied on larger statistics at UHE in AGASA) and also on the hybrid showers in AUGER will be useful to improve definitely the energy calibration of giant surface arrays.

We note also that a heavy composition will reduce the problems of inclined showers in AGASA, but will still be in conflict with the fluctuations of T_{max} measured with the Fly's Eye [29], [30].

REFERENCES

- [1] R. Sommers, rapporteur paper, 27th ICRC, Hamburg, 2001
- [2] P. Sokolsky, invited talk, XIV ISVHECRI, Weihai, China, August 15-22, 2006
- [3] J.N. Capdevielle and F. Cohen, Proc. 29th ICRC, Pune, 7, 59-62 (2005)
- [4] J.N. Capdevielle and F. Cohen, J.Phys.G 31, 1413-1419 (2005)
- [5] K. Shinozaki, invited talk, XIV ISVHECRI, Weihai, China, August 15-22, 2006
- [6] M. Nagano et al., Journal Phys. Soc. Japan, 53, 1667 (1984)
- [7] D. Heck, J. Knapp, J.N. Capdevielle, G. Schatz and T. Thouw FZK A report-6019 ed. FZK. The CORSIKA Air Shower Simulation Program, Karlsruhe (1998)
- [8] N.N. Kalmykov, S.S. Ostapchenko and A.I. Pavlov, Nuclear Physics B 52B, 17 (1997)
- [9] J.N. Capdevielle and F. Cohen, J.Phys. G, Nucl. Part. Phys., 31, 507-524 (2005)
- [10] F. Cohen, Ph. D. dissertation, Univ. Paris XI (2003)
- [11] P. D. G., Phys. Rev. D 54, 137 (1996)
- [12] A.M. Hillas, D.J. Marsden, J.D. Hollands and H.W. Hunter, Proc. 12th ICRC, Hobart, 3, 1001 (1971)
- [13] H.Y. Dai, K. Kasahara, Y. Matsubara, M. Nagano and M. Teshima, J. Phys. G, Nucl. Phys., 14 793, 805 (1988)
- [14] A. Lagutin, R.I. Raikin, N. Inoue and A. Misaki, J. Phys. G, 28, 1259 (2002)
- [15] H.J. Drescher, G. Farrar, M. Bleicher, M. Reiter, S. Soff and H. Stcker, Proc. 28th ICRC, Tsukuba, 2, 507 (2003).
- [16] M. Nagano et al., J.Phys.G, Nucl.Part.Phys., 18, 423 (1992)
- [17] S. Yoshida et al., J. Phys. G 20, 651-664 (1994)
- [18] S. Yoshida et al., Astrop. Phys. 3, 105 (1995)
- [19] G. Cocconi, EAS, vol. 46-1, Cosmic Rays, Handbuch der Physik, 223, Springer Verlag (1961)
- [20] A.V. Olinto, Proc. 28th ICRC, Tsukuba, 8, 299 (2003)
- [21] D. Bergman et al., HiRes Collaboration, Proc. 28th ICRC, Tsukuba, 1, 299 (2003)
- [22] R.W. Springer et al, HiRes Collaboration, Proc. 28th ICRC, Tsukuba, 1, 413 (2003)
- [23] J.N. Capdevielle, F. Cohen and K. Sanosyan, Proc. 28th ICRC, Tsukuba, 3, 1623 (2003)
- [24] J.N. Capdevielle, C. Le Gall, J. Gawin, I. Kurp, B. Szabelska, J. Szabelski and T. Wibig, Nuovo Cimento 25C 393, 424 (2002).
- [25] M. Takeda et al., (AGASA collaboration), 28th ICRC, Tsukuba, 1, 381 (2003)
- [26] A.A. Watson, "Astrophysical Aspects of the most energetic cosmic rays", 2, ed.M.Nagano, F. Takahara, World Scientific (1990)
- [27] C. Buttner et al., Proc. 28th ICRC, Tsukuba, 1, 33 (2003)
- [28] J. Lloyd-Evans, Proc. 22nd ICRC, Dublin, 5, 226-240 (1991)
- [29] P. Sokolsky, P. Sommers and B. Dawson, Physics Reports, 217, 5, 253-277 (1992)
- [30] J.N. Capdevielle and R. Attallah, J.Phys. G., Nucl. and Part. Phys., 21, 121-127 (1995)